Korean J. Chem. Eng., 33(6), 1799-1804 (2016)
DOI: 10.1007/s11814-016-0015-8

pISSN: 0256-1115
eISSN: 1975-7220

Enhanced activity of carbon-supported PdCo electrocatalysts toward electrooxidation of ethanol in alkaline electrolytes

Suenghoon Han*, Gyu-Sik Chae*, and Jae Sung Lee,†**

*Department of Chemical Engineering, Pohang University of Science & Technology (POSTECH), San 31 Hyoja-dong, Pohang 37673, Korea
**School of Energy & Chemical Engineering, Ulsan National University of Science & Technology (UNIST), 60 UNIST-gil, Ulsan 44919, Korea
(*Received 15 December 2015 • accepted 11 January 2016*)

Abstract−Carbon-supported Pd and PdCo (1 : 2, 1 : 1, 2 : 1 and 3 : 1) catalysts were synthesized by chemical reduction with $NaBH_4$. Their electrochemical properties were investigated by cyclic voltammetry, chronoamperometry and CO stripping voltammetry in alkaline electrolytes, and compared with commercial Pt/C and PtRu(1 : 1)/C catalysts. In electrochemical oxidation of ethanol in an alkaline electrolyte, marked improvements in the current density and onset potential were observed by incorporating Co into Pd/C to form PdCo/C alloy electrocatalysts. The best catalyst PdCo (1 : 1)/C showed performance superior to the commercial Pt/C or PtRu/C catalysts. It is shown that the incorporated Co facilitates the oxidation of strongly-adsorbed carbonaceous intermediate species on the surface of Pd by forming OH^- group and reacts away the intermediates from Pd surface. Thus, PdCo(1 : 1)/C catalyst is a promising anode catalyst for direct ethanol fuel cells with alkaline electrolytes.

Keywords: Palladium-cobalt Alloy, Electrocatalysts, Direct Ethanol Fuel Cells, Alkaline Electrolytes

INTRODUCTION

Direct alcohol fuel cells (DAFCs) have received much interest for their potential to become an alternative power source for automobiles and portable electronic devices such as cellular phones, lap tops and supplementary power generators [1,2]. Although methanol has been touted as the most promising fuel for DAFC, ethanol is regarded as a better option in terms of lower toxicity, higher boiling point, lower vapor pressure and higher energy density. In direct ethanol fuel cells (DEFCs), Pt or Pd-based catalysts have been used as anode electrocatalysts to oxidize ethanol [1,3-6]. In spite of arduous efforts, many limitations have been discovered in electrochemical oxidation of ethanol. First, complete oxidation of ethanol to CO_2 is not easy in acidic electrolyte at room temperature, because splitting the C-C bond in ethanol is a serious challenge. Another limitation in DEFCs is poisoning of the electrocatalyst by strongly adsorbed intermediates. Partial oxidation of ethanol produces carbonaceous species such as $(CH_3CO)_{ads}$ on the catalyst surface, which blocks the active catalytic sites from contacting fresh ethanol feed [7]. Thus, an effective anode catalyst for DEFC has to overcome these two limitations: splitting C-C bonds and removal of strongly adsorbed intermediates.

A possible solution is to carry out the ethanol oxidation in an alkaline electrolyte because the reaction has much faster kinetics than in acidic electrolytes [8,9]. Alkaline fuel cells (AFC) with hydrogen fuel and KOH(aq) electrolyte perform best of all known conventional hydrogen-oxygen fuel cells at low temperatures because of the facile kinetics both at the cathode and at the anode, and thus cheaper non-noble metal catalysts can be used. However, the practical application of AFC is limited because of the precipitation of metal carbonate/bicarbonate on reaction of KOH or NaOH electrolyte with CO_2 contamination in the oxidant gas stream in the electrolyte-filled pores of the electrodes, blocking pores and mechanically disrupting active layers. The use of anion exchange membranes (AEM) as a solid electrolyte, including no metal cations, prevents precipitation, and recent developments of fuel-cell grade AEM have revived the interest in all-solid alkaline membrane fuel cells without carbonate precipitation [8-10].

In alkaline electrolyte, Pd-based catalysts have shown much higher current densities than in acidic electrolyte [3], and thus Pd could be used instead of more expensive Pt in alkaline DEFCs. Unfortunately, Pd catalysts in alkaline DEFCs still have the two limitations mentioned above. Thus, to improve the activity and stability of Pd catalysts, binary or ternary alloys have been used as electrocatalysts for ethanol oxidation in alkaline DEFCs [8-15]. The Pd-Co alloys have been reported as catalyst for methanol oxidation, formic acid oxidation and oxygen reduction in acidic and alkaline electrolytes [16-21]. In the present work, we prepared carbon-supported Pd and Co alloy catalysts and applied them for the first time to ethanol oxidation in alkaline electrolyte. Small and well-distributed alloy particles were prepared by simple chemical reduction with $NaBH_4$, and those alloy catalysts show much higher oxidation current and more negative onset potential than monometallic Pd catalyst. On an optimized Pd-Co (1 : 1) alloy supported on carbon, Co exerted

†To whom correspondence should be addressed.
E-mail: jlee1234@unist.ac.kr
‡This article is dedicated to Prof. Seong Ihl Woo on the occasion of his retirement from KAIST.

dramatic effect on enhancing the generated current density as well as stability by reacting away the partially oxidized ethanol remnant.

EXPERIMENTAL

1. Catalyst Preparation

Carbon-supported Pd-based alloy catalysts were prepared by chemical reduction with $NaBH_4$ solution [2,22]. The amount of Pd was fixed at 20 wt% during the preparation, and the atomic ratio of Co to Pd was varied. Used metal precursors were palladium chloride ($PdCl_2$, Aldrich) and cobalt chloride hexahydrate ($CoCl_2 \cdot 6H_2O$, Aldrich). Quantitative amounts of the precursors and carbon black (Vulcan XC-72R, Cabot) were dissolved into 100 ml of water and the pH of the solution was adjusted at 4 by addition of 1.0 M NaOH. Under vigorous stirring, 100 ml of 0.08 M $NaBH_4$ solution was added rapidly into the solution. After stirring for 3 h, the resultant solution was filtered, washed with water and ethanol, and dried at 70 °C for 3 h. Commercial Pt/C and PtRu(1 : 1)/C (Etek, 20 wt% Pt or PtRu) catalysts were used as received as references.

2. Catalyst Characterization

The crystalline structures of the synthesized catalysts were determined by X-ray diffraction (XRD) using powder X-ray diffractometer (PANalytical, pw 3373/10 X'pert) with Cu Kα radiation. The working voltage and current were 40 kV and 30 mA, respectively. The 2θ angles were scanned over a range of 10 to 80° at a scan rate of 2.5° min^{-1}. The morphology of the synthesized nanoparticles on the carbon black was studied by high resolution transmission electron microscope (HR-[S]TEM, JEOL, JEM-2200FS, NCNT). For the quantitative analysis of the catalysts, inductively coupled plasma (ICP, Spectro Analytical Instruments, Flame Modula EOP) was used to investigate compositions of loaded metals.

3. Electrochemical Experiments

The cyclic voltammetry (CV) and chronoamperometry (CA) were carried out in a conventional three electrode cell containing aqueous solution of 1.0 M KOH and 1.0 M ethanol at room temperature using an IVIUM potentiostat. The CO stripping voltammetry was in 0.5 M KOH solution. Ag/AgCl (3 M NaCl, V=0.209 V *vs.* NHE) electrode and Pt wire were used as reference and counter electrodes, respectively. Working electrodes were prepared by dispersing 20 mg of catalyst into 2 ml of deionized water containing 40 µl of 5% Nafion solution, ultrasonicating for 30 min, and pipetting out 5 µl of slurry onto a glassy carbon electrode (0.0707 cm^2). After drying at 100 °C in an oven, 3 µl of Nafion solution was added to the glassy carbon electrode and dried again at 100 °C. Before conducting CV, CA, and CO stripping voltammetry, we purged the electrolyte with N_2 gas for 30 min to eliminate the remaining oxygenated species and polished the glassy carbon electrode with 0.3 µm and 0.05 µm alumina paste.

The CV tests were performed in a range of −0.9 V-0.2 V (*vs.* Ag/AgCl) at a scan rate of 50 mVs^{-1}. The positive scan limit was adjusted to 0.2 V to prevent further oxidation of Pd, Co and carbon. Chronoamperometry data were collected for 30 min at −0.5 V (*vs.* Ag/AgCl) in 1.0 M KOH and 1.0 M ethanol solution. For CO stripping voltammetry, CO gas (99.95%) was bubbled into N_2 gas-purged electrolyte for 30 min at −0.9 V (*vs.* Ag/AgCl) for CO adsorption on the catalyst. The solution was purged again with N_2 to remove CO gas in the electrolyte and potential scan was performed from −0.9 V to 0.2 V. Without specification, the potential in the present work was referred to the Ag/AgCl (3 M NaCl) electrode.

RESULTS AND DISCUSSION

1. Physicochemical Properties of Prepared Catalysts

The XRD patterns of Pd-based catalysts are compared in Fig. 1(A). All the synthesized catalysts show peaks corresponding to Pd metal of face-centered cubic (fcc) structure, and a broad diffraction peak at 20-25° in all catalysts is attributed to the (002) plane of the hexagonal structure of Vulcan XC-72 carbon used as the support. The $Co(OH)_2$ peaks at 19.11°, 32.56°, 38.78°, 51.51° and 58.09° are observed only in the catalyst of the highest Co loading, PdCo(1 : 2)/C. The Pd (220) peak of each catalyst was used to calculate the average Pd particle size with the Scherrer equation (with K value of 0.9) [23]. The average particle sizes of Pd/C, PdCo(3 : 1)/C, PdCo(2 : 1)/C and PdCo(1 : 1)/C were determined to be 3.2 nm,

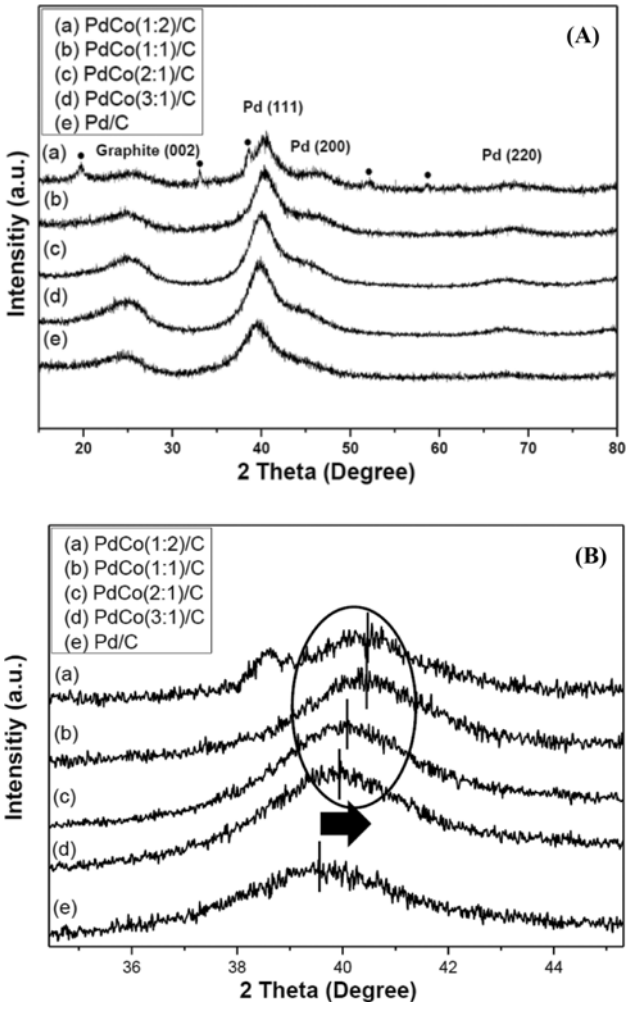

Fig. 1. XRD patterns of synthesized catalysts: (A) The whole scans for each catalyst. The peaks due to $Co(OH)_2$ are indicated for PdCo(1 : 2)/C. (B) Shifts of the Pd(111) peak to higher angles by alloy formation with Co.

3.6 nm, 3.7 and 3.9 nm, respectively. The PdCo(1 : 2)/C catalyst was excluded due to the superposition of $Co(OH)_2$ peaks and Pd peaks. All the PdCo/C alloy catalysts showed the systematic higher angle shift of (111) peak as shown in Fig. 1(B), and as the Co content was higher, the larger was the shift from that of Pd/C. This indicates lattice contraction due to the incorporation of Co into Pd lattice [24]. In the XRD analysis, Co or $Co(OH)_2$ peaks were not observed when atomic ratio of Co/Pd was below unity. PdCo(1 : 2)/C showed both the peak shift and the presence of $Co(OH)_2$. This reveals that incorporated Co forms alloy at low Co contents as observed by the systematic peak shift and that the excess Co forms $Co(OH)_2$ as an impurity phase at the high Co content.

TEM images of the synthesized Pd/C and PdCo(1 : 1)/C are presented in Fig. 2(a)-(d). It is evident that Pd and PdCo(1 : 1) particles are well dispersed on carbon and the average particle sizes of Pd/C and PdCo(1 : 1) are 2.9 nm and 3.1 nm, respectively, which are a little smaller than the particle sizes estimated by XRD with the Scherrer equation. Note that these catalysts were prepared in the presence of NaOH. When Pd and PdCo(1 : 1) particles were synthesized without NaOH, the metal particles aggregated with each other and the size became larger as shown in Fig. 2(e), (f). These small and well-dispersed nanoparticles result from the adjustment of solution pH with NaOH because palladium (II) cations ionized in the solution are not uniformly adsorbed on carbon at highly acidic conditions. Kim et al. [25] reported that well-dispersed Pd particles resulted from a strong interaction between Pd and the support at pH 10, but our results showed that pH 4 was also effective. Hence, we can conclude that Pd or PdCo alloy particles of ca. 3 nm are uniformly dispersed on carbon support.

The surface of catalysts was further investigated by XPS analysis. The binding energies of Pd $3d_{3/2}$ and Pd $3d_{5/2}$ of PdCo(1 : 1)/C are 340.8 eV and 335.5 eV as shown in Fig. 3(a), which are 0.1 eV higher than that of Pd/C catalysts prepared in this work. The shift of binding energy may result from the interaction between Pd with Co atoms, which decreases 3d electron density of Pd in PdCo(1 : 1)/C catalyst [26]. The oxidized state of Pd is also observed at 342.0 eV and 336.5 eV due to the partial oxidation of Pd on the catalyst surface. Higher binding energies of Co $2p_{1/2}$ and Co $2p_{3/2}$ of PdCo(1 : 1)/C catalyst were also observed as compared to metallic Co. The results show that Co on the surface of the catalyst has oxidation state mainly of Co^{2+} such as $Co(OH)_2$ and CoO. Thus, XPS results also indicate the formation of PdCo metallic alloy although the surface is partly oxidized. Some segregated Co^{2+} phases are also present

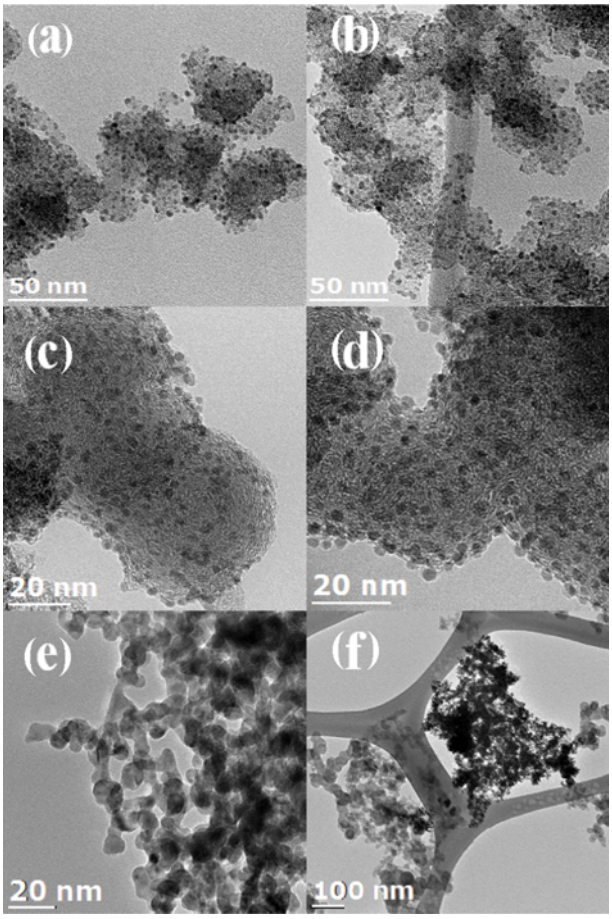

Fig. 2. TEM images of catalysts synthesized with NaOH: (a), (b) Pd/C; (c), (d) PdCo(1 : 1)/C. Without NaOH: (e) Pd/C; (f) PdCo(1 : 1)/C.

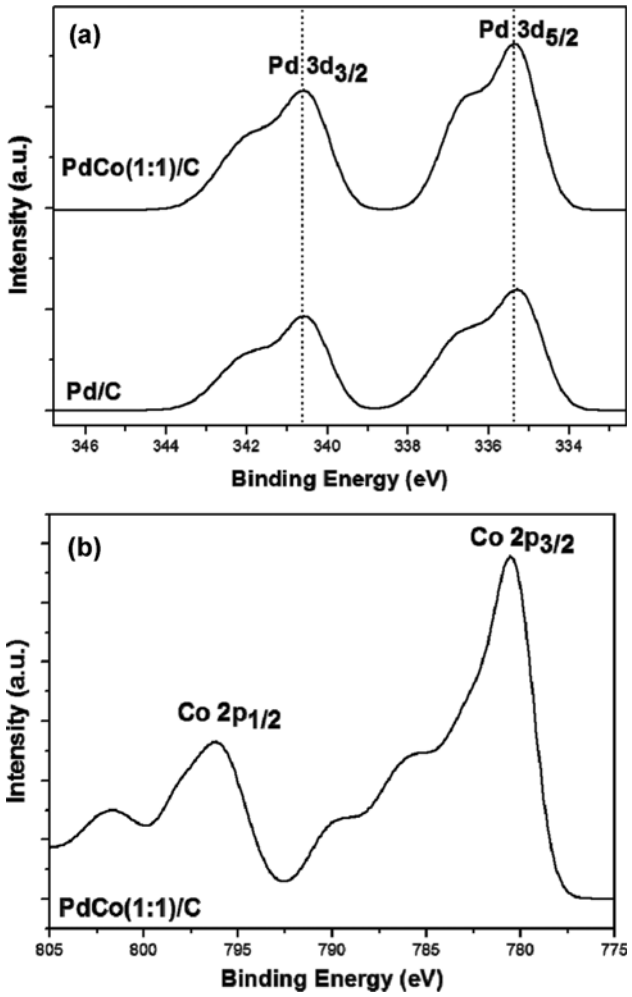

Fig. 3. XPS spectra of Pd 3d (a) and Co 2p (b) of PdCo(1 : 1)/C and Pd/C.

Table 1. ICP results of the catalysts

Catalyst	Element	Wt%	Molar ratio of Pd to Co
Pd/C	Pd	18.6	
PdCo(3 : 1)/C	Pd	18.9	4.8
	Co	2.2	
PdCo(2 : 1)/C	Pd	18.7	2.7
	Co	3.8	
PdCo(1 :1)/C	Pd	17.2	1.2
	Co	7.7	

on the surface, especially for catalysts of high Co content.

To confirm the actual composition of Pd and Co in the catalysts, ICP analysis was performed and the results are presented in Table 1. The actual atomic ratios of PdCo(3 : 1), PdCo(2 : 1) and PdCo(1 : 1) are 4.8 : 1, 2.7 : 1 and 1.2 : 1, respectively. The results show preferential loss of Co during the synthesis, but in case of PdCo(1 : 1) with the atomic ratio of 1.2 : 1, the loss was minimal.

2. Electrochemical Performance of Alloy Catalysts

To investigate the electrochemical performance of the prepared catalysts, CV measurements were carried out in 1.0 M KOH - 1.0 M ethanol solution, and the results are presented in Fig. 4(a). During the forward scan, ethanol started to be oxidized from −0.8 V to −0.7 V and CV showed broad maximum current density because the surface of catalysts was covered with products and intermediate. A sharper peak of ethanol oxidation is observed in backward scan due to the removal of the carbonaceous species not completely oxidized during the forward scan [12]. Therefore, the two maxima represented a typical ethanol oxidation CV on Pd-based electrocatalysts. The onset potentials of ethanol oxidation on Pd/C, PdCo(1 : 1)/C and PdCo(1 : 2)/C were −0.78 V, −0.84 V and −0.67 V, respectively. The onset potential of PdCo(1 : 2)/C was much higher than that of PdCo(1 : 1)/C because Co was not fully incorporated with Pd and formed $Co(OH)_2$ on the surface of catalysts. The current density of forward scan increased according to the amount of the incorporated Co; PdCo(1 : 2)/C>PdCo(1 : 1)/C>PdCo(2 : 1)/C>PdCo(3 : 1)/C>Pd/C. Thus, alloy catalysts showed much better electrocatalytic activity of ethanol oxidation in alkaline conditions than monometallic Pd/C [24]. In addition, the CV results of PdCo (1 : 1)/C and commercial Pt/C and PtRu/C catalysts are compared in Fig. 4(b). Pd/C catalyst shows comparable onset potential and current density to commercial Pt/C catalyst and this reveals that Pd-based catalysts could be used as electrocatalyst in alkaline electrolyte instead of expensive Pt-based catalysts commonly used in acid electrolyte. Commercial PtRu(1 : 1)/C shows much better catalytic activity of ethanol oxidation than Pt/C and Pd/C catalyst. However, our PdCo(1 : 1)/C catalyst still shows the highest current density than that of all commercial catalysts and its onset potential (−0.84 V) is comparable to that of PtRu(1 : 1)/C (−0.87 V). The results demonstrate that our PdCo/C alloy catalysts outperform all the commercial fuel cell catalysts for electrochemical oxidation of ethanol in alkaline electrolyte.

To investigate long-term stability of our PdCo alloy catalysts, the CA test was conducted at −0.5 V in 1.0 M KOH - 1.0 M ethanol solution for the PdCo(1 : 2, 3 : 1, 2 : 1 and 1 : 1)/C and Pd/C catalysts. As shown in Fig. 5, all the catalysts feature the decay of current density during the first 5 min due to the strongly adsorbed

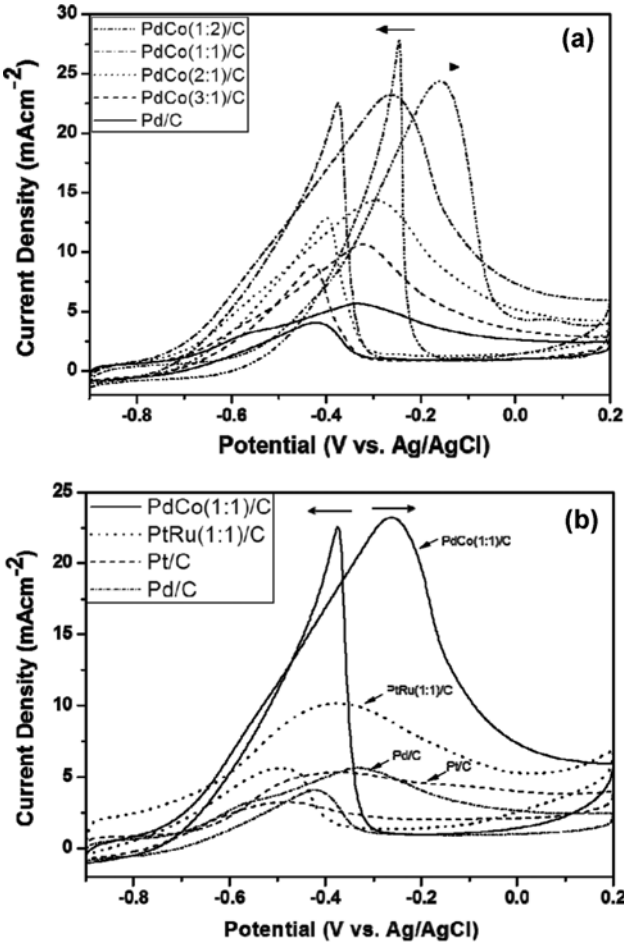

Fig. 4. Cyclic voltammogram of ethanol oxidation on the synthesized PdCo/C catalysts (a) and the commercial catalysts (b) in 1.0 M KOH - 1.0 M ethanol solution.

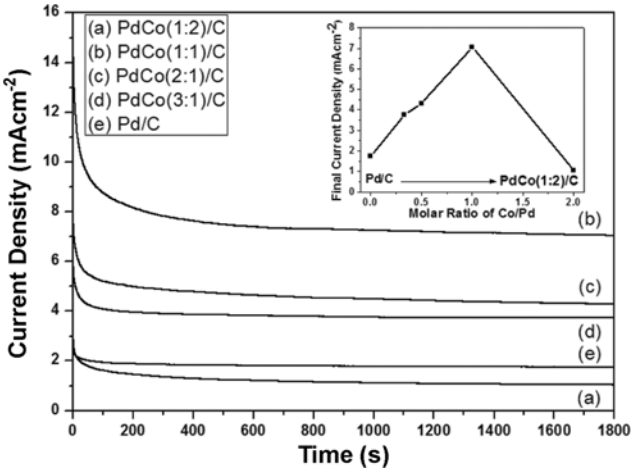

Fig. 5. Chronoamperometry results of ethanol oxidation on synthesized catalysts in 1.0 M KOH - 1.0 M ethanol solution at −0.5 V (*vs.* Ag/AgCl).

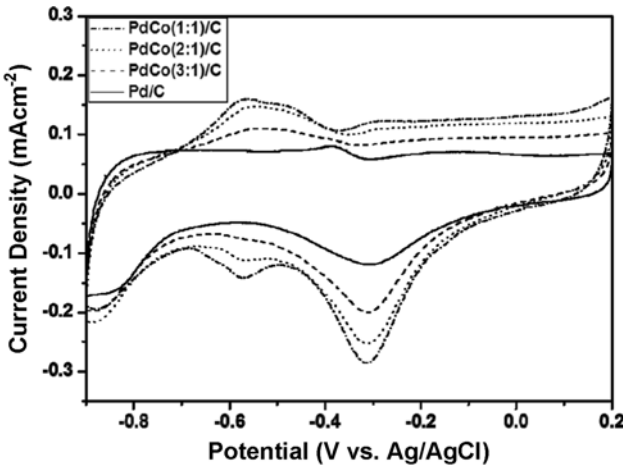

Fig. 6. The 20th cycle of cyclic voltammetry results of synthesized PdCo/C and Pd/C catalysts in 0.5 M KOH solution.

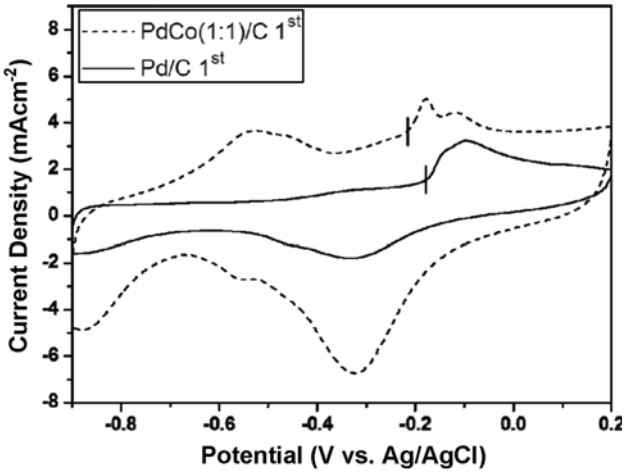

Fig. 7. The 1st cycle of CO stripping voltammogram of Pd/C and PdCo(1 : 1)/C in 0.5 M KOH solution.

intermediates and the decay slows down after 5 min [11]. Like the CV results, the current densities of ethanol oxidation on PdCo(1 : 1)/C were higher than those for the other catalysts. In the inset of Fig. 5, the final current density at 1,800 s is plotted against the molar ratio of Co/Pd. A volcano-type performance curve is observed with a maximum for PdCo(1 : 1)/C. Thus the final current increased almost linearly with Co content for Co/Pd of below unity. Yet further addition of Co deteriorated the performance probably because of surface segregation of excess Co in the form of $Co(OH)_2$.

The complete cleavage of C-C bond of ethanol is not easy on Pt and Pd-based catalysts [3]. A strongly adsorbed carbonaceous species such as $(CH_3CO)_{ads}$ is produced rather than complete oxidation to CO_2 during the electrooxidation of ethanol [27]. Such fouling by-products should be removed as fast as possible because they cover active sites of catalysts and inhibit adsorption of fresh ethanol. According to the previous results, more OH^- ions can adsorb on the incorporated transition metal at lower potentials than Pd, and the adsorbed OH^- ions oxidize the adsorbed intermediates [24]. This phenomenon is also observed in PdCo(1 : 1, 2 : 1 and 3 : 1) catalysts as presented in Fig. 6 that shows the 20th cycle of cyclic voltammetry results of synthesized catalysts in 0.5 M KOH solution. When Co is incorporated into Pd, a broad peak appears at −0.6 V, which can be assigned to the adsorption of OH^- ions on the surface of PdCo(1 : 1, 2 : 1 and 3 : 1)/C catalysts. Zhang et al. [27] suggested that the rate determining step of ethanol oxidation is removal of $(CH_3CO)_{ads}$ from the surface of Pd. The supply of more OH^- ions facilitated by the incorporated Co on the surface of catalyst can promote the suggested rate determining step and thus the rate of overall reaction. Based on these ideas, a modified rate determining step could be written as follows:

$$Pd\text{-}(CH_3CH_2OH)_{ads} + 3OH^- \rightarrow Pd\text{-}(CH_3CO)_{ads} + 3H_2O + 3e^- \quad (1)$$

$$Pd\text{-}(CH_3CO)_{ads} + PdCo\text{-}OH_{ads} \rightarrow Pd\text{-}(CH_3COOH)_{ads} + PdCo \quad (2)$$

$$Pd\text{-}(CH_3COOH)_{ads} + OH^- \rightarrow Pd + CH_3COO^- + H_2O \quad (3)$$

To verify the ability to remove intermediates with the incorporated Co, CO (one of strongly-adsorbed carbonaceous species) stripping test was performed in 0.5 M KOH solution. Fig. 7 shows the voltammogram of CO oxidation on Pd/C and PdCo(1 : 1)/C. The anodic peak results from oxidation of the adsorbed CO monolayer on the surface of the catalysts [13]. The onset potential of PdCo(1 : 1)/C apparently shifts to negative potential by approximately 40 mV from that of Pd/C catalyst. This could be understood by the role of Co in PdCo alloy catalysts, which facilitates oxidative removal of poisoning intermediates from the active Pd surface. Therefore, addition of Co to Pd/C catalyst forming PdCo alloy promotes the activity and stability of electrochemical ethanol oxidation in alkaline electrolyte.

CONCLUSIONS

Pd/C and PdCo(1 : 2, 1 : 1, 2 : 1 and 3 : 1)/C electrocatalysts were synthesized by chemical reduction method with $NaBH_4$ and their physicochemical and electrochemical properties were characterized by XRD, TEM, ICP, CV, CA and CO stripping test. The characterization revealed that the PdCo alloys were successfully prepared with small and uniform particle sizes of ca. 3 nm that were well dispersed on carbon support. In the CV result, the addition of Co into Pd catalysts drastically enhanced catalytic activity of Pd for ethanol oxidation in alkaline electrolyte. The optimized PdCo(1 : 1)/C catalyst outperformed the commercial catalysts Pt/C and PtRu/C in CV test in alkaline electrolyte. The onset potential of PdCo(1 : 1)/C was also comparable to that of commercial PtRu(1 : 1)/C. It was shown that the incorporated Co facilitated the oxidation of strongly-adsorbed carbonaceous intermediate species on the surface of Pd by forming OH^- group and reacts away the intermediates from Pd surface. Thus, PdCo(1 : 1)/C catalyst could be a promising anode catalyst for DEFCs with alkaline electrolyte.

ACKNOWLEDGEMENTS

This research was supported by Brain Korea Plus Program of Ministry of Education, and Korea Center for Artificial Photosynthesis (KCAP, No. 2009-0093880) funded MSIP, and Project No.

10050509 funded by MOTIE of Republic of Korea. This work was also supported by Ulsan National Institute of Science and Technology.

REFERENCES

1. J. Otomo, S. Nishida, H. Kato, H. Nagamoto and Y. Oshima, *ECS Trans*., **16**, 1275 (2008).
2. D. H. Youn, S. Han, G. Bae and J. S. Lee, *Electrochem. Commun*., **13**, 806 (2011).
3. L. Ma, D. Chu and R. Chen, *Int. J. Hydrogen Energy*, **37**, 11185 (2012).
4. F. Alcaide, G. Álvarez, P. L. Cabot, H.-J. Grande, O. Miguel and A. Querejeta, *Int. J. Hydrogen Energy*, **36**, 4432 (2011).
5. N. Kakati, J. Maiti, S. H. Lee and Y. S. Yoon, *Int. J. Hydrogen Energy*, **37**, 19055 (2012).
6. W. Wei and W. Chen, *J. Power Sources*, **204**, 85 (2012).
7. Y.-C. Wei, C.-W. Liu, W.-D. Kang, C.-M. Lai, L.-D. Tsai and K.-W. Wang, *J. Electroanal. Chem*., **660**, 64 (2011).
8. E. J. Lim, H. J. Kim and W. B. Kim, *Catal. Commun*., **25**, 74 (2012).
9. E. J. Lim, Y. Kim, S. M. Choi, S. Lee, Y. Noh and W. B. Kim, *J. Mater. Chem. A*, **3**, 5491 (2015).
10. T. S. Almeida, L. M. Palma, P. H. Leonello, C. Morais, K. B. Kokoh and A. R. De Andrade, *J. Power Sources*, **215**, 53 (2012).
11. Y.-Y. Feng, Z.-H. Liu, Y. Xu, P. Wang, W.-H. Wang and D.-S. Kong, *J. Power Sources*, **232**, 99 (2013).
12. T. Maiyalagan and K. Scott, *J. Power Sources*, **195**, 5246 (2010).
13. K. Miecznikowski and P. J. Kulesza, *J. Power Sources*, **196**, 2595 (2011).
14. R. M. Modibedi, T. Masombuka and M. K. Mathe, *Int. J. Hydrogen Energy*, **36**, 4664 (2011).
15. T. Ramulifho, K. I. Ozoemena, R. M. Modibedi, C. J. Jafta and M. K. Mathe, *Electrochim. Acta*, **59**, 310 (2012).
16. Q. Tang, L. Jiang, Q. Jiang, S. Wang and G. Sun, *Electrochim. Acta*, **77**, 104 (2012).
17. D.-S. Kim, J.-H. Kim, I.-K. Jeong, J. K. Choi and Y.-T. Kim, *J. Catal*., **290**, 65 (2012).
18. X. Wang and Y. Xia, *Electrochem. Commun*., **10**, 1644 (2008).
19. D. Morales-Acosta, J. Ledesma-Garcia, L. A. Godinez, H. G. Rodríguez, L. Álvarez-Contreras and L. G. Arriaga, *J. Power Sources*, **195**, 461 (2010).
20. A. Serov, T. Nedoseykina, O. Shvachko and C. Kwak, *J. Power Sources*, **195**, 175 (2010).
21. J. Yang, C. H. Cheng, W. Zhou, J. Y. Lee and Z. Liu, *Fuel Cells*, **10**, 907 (2010).
22. D. H. Lim, D. H. Choi, W. D. Lee, D. R. Park and H. I. Lee, *Electrochem. Solid State Lett*., **10**, B87 (2007).
23. V. Radmilovic, H. A. Gasteiger and P. N. Ross, *J. Catal*., **154**, 98 (1995).
24. Y. Wang, X. Wang and C. M. Li, *Appl. Catal. B*, **99**, 229 (2010).
25. D. H. Kim, S. I. Woo and O. B. Yang, *Appl. Catal. B*, **26**, 285 (2000).
26. Y. W. Tang, Y. Chen, P. Zhou, Y. M. Zhou, L. D. Lu, J. C. Bao and T. H. Lu, *J. Solid State Electrochem*., **14**, 2077 (2010).
27. Z. Zhang, L. Xin, K. Sun and W. Li, *Int. J. Hydrogen Energy*, **36**, 12686 (2011).